Differences in straggling for positrons and electrons

D. P. Heddle*
Nuclear Physics Laboratory, University of Illinois, Champaign, Illinois 61820

Leonard C. Maximon
National Institute of Standards and Technology, Gaithersburg, Maryland 20899
(Received 9 June 1988)

A satisfactory analysis of the physics of straggling was first given by Landau, who approximated the electron-electron cross section for hard collisions by the Rutherford cross section. Data analysis computer codes continue to use the distribution derived by Landau to calculate the energy lost by electrons because of straggling. We have performed a study of straggling distributions incorporating Møller and Bhabha cross sections to evaluate the precision of (e,e') analyses that use the Rutherford-based Landau formula. In addition, the calculation of the e^+ straggling distribution is relevant to the analysis of experiments that have been proposed to study dispersive effects in nuclear electromagnetic processes by comparing results obtained from e^- and e^+ scattering from identical nuclei. Measuring differences in such cross sections requires a high degree of confidence in the data analysis. Since accuracies in cross sections on the order of a few percent are required, any differences in energy-loss mechanisms of the same order must be taken into account. In this work, we study the differences in positron and electron straggling at energies of present-day interest.

I. INTRODUCTION

Straggling refers to the distribution in energies that results when a swift charged particle passes through a thin target. The distribution arises because the energy-loss process is inherently statistical. The definition of a thin target is that the incident particles will undergo, on the average, one "hard" collision where significant (to be quantified later) energy is transferred. Thus, there is no chance for an averaging process to occur, and an asymmetric distribution of energy losses results.

A satisfactory analysis of the physics of straggling was first given by Landau.[1] Landau correctly identified the regime in which the screening by the bound atomic electrons in the target was important and the importance of "hard" collisions for the energy-loss region of the straggling distribution. In order to simplify the calculation of the hard collisions with the atomic electrons, Landau approximated the electron-electron cross section by the Rutherford cross section. Many experiments use the distribution derived by Landau to calculate the energy lost by electrons due to straggling. A review of Landau straggling for a single absorber, and an exhaustive list of references, can be found in a recent article by Bichsel.[2]

We have studied how the straggling distributions are altered when, instead of approximating the electron-electron and positron-electron cross sections by the Rutherford cross section, one uses the more precise Møller cross section (for an e^- beam) or the Bhabha cross section (for an e^+ beam). Part of the motivation for this study is simply to understand the precision of the Rutherford-based analyses of straggling. Further motivation stems from the precision analysis required by proposed experiments to measure dispersion corrections in high-energy electron scattering from atomic nuclei. It has been known for some time that dispersion corrections are different for the scattering of electrons and positrons from identical nuclei.[3,4] The differences are expected to appear outside the diffraction minima, where the real part of the static amplitude, which is first order in the Coulomb potential, dominates. Such effects are seen in the coupled-channel calculations of Ravenhall and Mercer.[5] However, only recently has the positron beam current and energy resolution improved to the point where the corresponding experiments are feasible. Experiments have been performed to study these differences on ^{12}C and ^{208}Pb at Saclay.[6] Dispersion corrections are generally believed to be of the order of a few percent; in order to infer their presence in measured electron and positron spectra we must be able to account for differences in energy-loss mechanisms for electrons and positrons to a very high level of accuracy. Rohrlich and Carlson[7] have made order-of-magnitude estimates for electron-positron differences in the collisional average energy-loss, straggling, and multiple-scattering effects at low energies ($\lesssim 10$ MeV). In certain cases, they found differences sizable enough to be of concern. In their work, approximations for cross sections based on expansions in the fractional energy transfer were used. Here, we extend their analysis of the straggling problem to higher energies and incorporate the exact Bhabha cross section and a more accurate approximation for the Møller cross section.

II. ANALYSIS

In this section, we will review Landau's analysis and describe how we incorporated the Møller and Bhabha cross sections into the same framework.

A. Preliminaries

Following the lead of Rohrlich and Carlson,[7] we describe straggling in terms of the *fractional* energy loss

$$\epsilon=\frac{\delta E}{T} , \tag{1}$$

where T is the kinetic energy of the incident particle and δE is the energy lost while scattering from an atomic electron. Note that ϵ has the physical limits

$$0\leq\epsilon\leq\begin{cases}\frac{1}{2} & \text{Møller scattering}\\ 1 & \text{Bhabha scattering} .\end{cases} \tag{2}$$

The limit of $\frac{1}{2}$ in the case of Møller scattering is due to the indistinguishability of the incident and target electrons; after the collision, the primary electron is identified as the one with the greater energy. It is useful to define the quantity.

$$\chi=\frac{2\pi r_0^2 mc^2}{\beta^2} , \tag{3}$$

where $r_0=e^2/(mc^2)$ is the classical electron radius, $\beta=v/c$, and e, m, and v are the charge, mass, and velocity of the incident particle.

The characteristic fractional energy transfer, above which collisions are "hard," turns out to be[8]

$$\zeta=\frac{xN_0\chi}{T}\frac{\Sigma_i n_i Z_i}{\Sigma_i n_i A_i} , \tag{4}$$

where x is the target thickness, with dimension $(M\cdot L^{-2})$ (e.g., gm/cm^2), N_0 is Avogadro's number, and the sums are over constituent atomic numbers and masses weighted by the constituent fraction n_i. All the target information is contained in the dimensionless quantity ζ. This makes it convenient to use ζ as an independent variable.

The cross sections for the scattering of electrons or positrons from free electrons can be written in the form

$$\frac{d\sigma}{d\epsilon}=\frac{\chi}{T}g(\epsilon) . \tag{5}$$

In this paper, we often refer to the term $g(\epsilon)$ itself as the cross section. The original paper by Landau[1] approximated the electron-electron scattering cross section with the Rutherford cross section

$$g_R(\epsilon)=\frac{1}{\epsilon^2} . \tag{6}$$

To correct Landau's calculation for the more exact Møller (electron-electron) and Bhabha (positron-electron) cross sections we can write

$$g(\epsilon)=\frac{1}{\epsilon^2}+c(\epsilon)=g_R(\epsilon)+c(\epsilon) , \tag{7}$$

where the term $c(\epsilon)$ will be written $c_M(\epsilon)$ for Møller and $c_B(\epsilon)$ for Bhabha scattering; the corrections are discussed below.

B. Review of Landau's analysis

The straggling distribution is $f(x,\Delta)$, where $f(x,\Delta)d\Delta$ is the probability that the incident particle has lost a fractional energy between Δ and $\Delta+d\Delta$ after traversing a distance x inside the target. Landau showed that a general solution for $f(x,\Delta)$ is

$$f(x,\Delta)=\frac{1}{2\pi i}\int_{\sigma-i\infty}^{\sigma+i\infty}\exp\left[p\Delta-\zeta\int_0^{\epsilon_{\max}}w(\epsilon)(1-e^{-p\epsilon})d\epsilon\right]dp , \tag{8}$$

where σ is an arbitrary real constant, $w(\epsilon)$ is the probability that an incident particle will lose fractional energy ϵ in a single collision, and $\epsilon_{\max}$ is the maximum energy loss given by Eq. (2). Note that when the energy transfer is large enough that we can safely ignore the atomic binding, $w(\epsilon)$ in Eq. (8) goes over into the free-electron scattering cross section $g(\epsilon)$.

Landau recognized on physical grounds that the only values of the dummy variable p that contribute significantly to the integral in Eq. (8) are

$$\frac{1}{\epsilon_{\max}}\ll p\ll\frac{1}{\epsilon_0} , \tag{9}$$

where the characteristic fractional energy transfer ϵ_0 roughly delimits the region where we can make the approximation that the atomic electrons are free. A precise value for ϵ_0 will not be important. It is of the order

$$\epsilon_0\approx\frac{\bar{I}}{T}\approx\frac{10^{-5}Z}{T} , \tag{10}$$

where T is measured in MeV and $\bar{I}$ is average ionization energy of an atom with atomic number Z in eV, which is given approximately by

$$\bar{I}\approx 9.1Z(1+1.9Z^{-2/3})\text{ eV}\approx 10Z\text{ eV} . \tag{11}$$

For completeness we note that for composite targets Eq. (11) is replaced by[8]

$$\ln\bar{I}=\Sigma_i f_i\ln\bar{I}_i ,$$

where

$$f_i=\frac{n_i Z_i}{\Sigma_i n_i Z_i} , \tag{12}$$

and, as before, n_i is the constituent fraction. Landau also showed that Eq. (9) is equivalent to

$$\epsilon_0\ll\zeta\ll\epsilon_{\max} . \tag{13}$$

Since ζ depends explicitly on target parameters and the

incident energy, this equation can be viewed as determining whether or not the Landau analysis is applicable. To see this more clearly, consider the following order-of-magnitude estimates. First, we have the trivial estimate $\epsilon_{\max} \approx 1$. Secondly, using the approximations $\beta \approx 1$ and $A \approx 2Z$ then Eqs. (3) and (4) give

$$\zeta \approx \frac{x}{10T} , \tag{14}$$

where x is in gm/cm^2 and T is in MeV. Taken together with Eq. (13), these estimates establish a restriction on the target thickness

$$10^{-4}\, Z \ll x \ll 10T . \tag{15}$$

Of course, this inequality is meaningful only if the implied units for x and T are not forgotten.

Landau noted that Eq. (9) allows us to define an ϵ_1 such that $\epsilon_1 > \epsilon_0$ while at the same time we still have $p \ll 1/\epsilon_1$. Then the integral in the exponent of Eq. (8), which we call I_L, can split into two parts:

$$I_L = \int_0^{\epsilon_{\max}} w(\epsilon)(1-e^{-p\epsilon})d\epsilon$$
$$= \int_0^{\epsilon_1} w(\epsilon)(1-e^{-p\epsilon})d\epsilon + \int_{\epsilon_1}^{\epsilon_{\max}} g_R(\epsilon)(1-e^{-p\epsilon})d\epsilon . \tag{16}$$

In the first region, the definition of ϵ_1 permits the simplifying approximation $(1-e^{-p\epsilon}) \approx p\epsilon$. That integral then represents the average energy loss over the low-energy region and has a well-known result[9] which is incorporated below in Eq. (17). In the second region, the inequality of Eq. (9) and the behavior of $g_R(\epsilon)$ imply that the upper limit of the integral can be extended to ∞. The result obtained by Landau is

$$I_L = p[1 - \ln\epsilon' p - \Gamma + \mathcal{O}(\epsilon_1 p)] , \tag{17}$$

where $\Gamma = 0.577\ldots$ is the Euler constant. ϵ' is defined by

$$\ln\epsilon' = \ln\frac{\bar{I}^2}{2m\gamma^2\beta^2 T} + \beta^2 , \tag{18}$$

where $\gamma = (1-\beta^2)^{-1/2}$ is the relativistic factor.

It is easy to see that this evaluation of I_L leads to the result

$$f(x,\Delta) = \frac{1}{\zeta}\frac{1}{2\pi i}\int_{\sigma-i\infty}^{\sigma+i\infty} e^{\lambda u + u\ln u} du , \tag{19}$$

where the dimensionless variable λ is given by

$$\lambda = \frac{\Delta}{\zeta} + \Gamma - 1 + \ln\frac{\epsilon'}{\zeta} . \tag{20}$$

An important result is that we can write

$$f(x,\Delta) = \frac{1}{\zeta}\Phi(\lambda) , \tag{21}$$

where $\Phi(\lambda)$ is a universal function independent of target and beam parameters. Two important phenomenological results obtained from numerical tabulation of the universal function are[10,11]

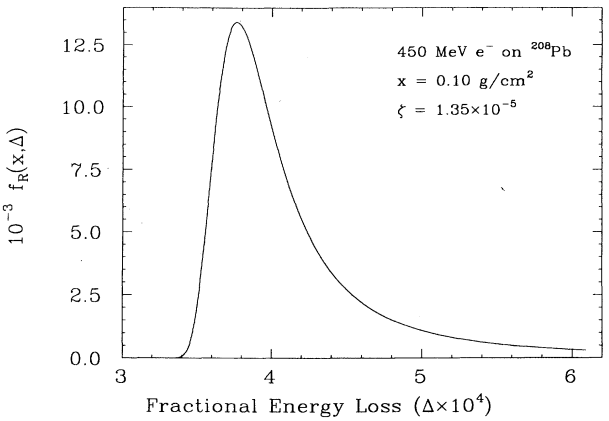

FIG. 1. Standard (Rutherford) Landau straggling for 450-MeV electrons on ^{208}Pb with a target thickness of 0.01 gm/cm^2.

$$\Delta_{MP} \approx \zeta\left[\ln\frac{\zeta}{\epsilon'} + 0.198\right] , \tag{22}$$

where Δ_{MP} is the most-probable energy loss and

$$W \approx 4.02\zeta , \tag{23}$$

where W is the full width at half maximum (FWHM) of the distribution. It is of interest to see how these quantities differ from their Rutherford values for the Bhabha and Møller cross sections.

It is of both historical and practical interest to note that the original Landau result for Δ_{MP} is incorrect; it contains a term 0.37ζ rather than the 0.198ζ appearing in Eq. (22). Landau deferred the numerical evaluation of Eq. (19) to the Calculation Bureau of the Mathematical Institute of the Academy of Sciences of the U.S.S.R. Despite its relatively simple appearance it is not a trivial integral, even when using modern computers. One can imagine the difficulty in its evalution using the computational resources available in 1944.

An example of a "standard" (i.e., Rutherford cross section) Landau straggling distribution is shown in Fig. 1. In the following sections, we examine the corrections to Landau straggling when the Møller or Bhabha cross section is used in place of the Rutherford cross section, and compare the straggling for incident electrons with that for positrons.

C. Incorporating the Bhabha and Møller cross sections

The problem at hand is to modify Landau's calculation of the integral in Eq. (8) to reflect the appropriate cross section. We can write the integral as

$$I = \int_0^{\epsilon_{\max}} w(\epsilon)(1-e^{-p\epsilon})d\epsilon$$
$$= I_L + \int_{\epsilon_1}^{\epsilon_{\max}} c(\epsilon)(1-e^{-p\epsilon})d\epsilon = I_L + I_C . \tag{24}$$

Clearly I_C is the correction term for cross sections other than Rutherford. Note that we have assumed that the

low-energy portion of the integral ($\epsilon<\epsilon_1$) is unchanged. This is reasonable since that is the regime of scattering from bound electrons and it should not be affected by our choice of free-electron cross section. Also, we have restored the upper limit in the correction term to its "proper" value of $\epsilon_{\max}$. The correction term I_C modifies Eq. (19) to

$$f(x,\Delta)=\frac{1}{\zeta}\frac{1}{2\pi i}\int_{\sigma-\infty}^{\sigma+\infty}e^{\lambda u+u\ln u-\zeta I_C(u/\zeta)}du\ , \tag{25}$$

where $u=\zeta p$. This equation shows that we can no longer factor out the target dependence, i.e., there is no longer a universal function $\Phi(\lambda)$. However, it is still useful to write $f(x,\Delta)$ as

$$f(x,\Delta)=\frac{1}{\zeta}\Phi(\lambda,\zeta)\ , \tag{26}$$

1. *Møller formulation*

Referring to Eq. (7), the correction term for the Møller cross section[12] is

$$c_M(\epsilon)=\left[\frac{\gamma-1}{\gamma}\right]^2-\frac{2\gamma-1}{\gamma^2}\frac{1}{\epsilon}-\frac{2\gamma-1}{\gamma^2}\frac{1}{1-\epsilon}+\left[\frac{1}{1-\epsilon}\right]^2 . \tag{27}$$

Inserting this into the correction term of Eq. (24) and using the table of integrals from the Appendix, we get

$$I_C^M=2+c_0\left[\frac{1}{2}-\frac{1}{p}\right]+c_1(\Gamma+\ln p)-(c_1+p)J(p)\ , \tag{28}$$

where $u=\zeta p$ and

$$c_0=\left[\frac{\gamma-1}{\gamma}\right]^2\ ,\qquad c_1=\frac{2\gamma-1}{\gamma^2}\ , \tag{29}$$

and

$$J(p)=\int_{\epsilon_1}^{\epsilon_{\max}}\frac{e^{-p\epsilon}}{1-\epsilon}d\epsilon\ .$$

It is easy to see that a very good approximation for $J(p)$ in the region $1/\epsilon_{\max}\ll p\ll 1/\epsilon_1$ is

$$J(p)\approx\frac{1}{p}+\frac{1}{p^2}+\frac{2}{p^3}+\frac{6}{p^4}\ . \tag{30}$$

Using this result we can write I_C^M as

$$I_C^M=\frac{1}{\zeta}\left[m_{-1}\ln\frac{u}{\zeta}+\sum_{n=0}^{3}m_n\left[\frac{\zeta}{u}\right]^n\right]\ , \tag{31}$$

where the m_n are defined by

$$\begin{aligned}m_{-1}&=c_1\ ,\\ m_0&=\tfrac{1}{2}c_0+2+c_1\Gamma\ ,\\ m_1&=-(c_0+c_1+1)\ ,\\ m_2&=-(c_1+2)\ ,\end{aligned} \tag{32}$$

and

$$m_3=-(2c_1+6)\ .$$

The reason for transforming I_C^M into the form given by Eq. (31) will become apparent in the next section.

Rohrlich and Carlson[7] used only the $1/\epsilon$ term from Eq. (27) in approximating the Møller cross section. Our use of Eq. (30) amounts to adding on an approximation of the terms that they omitted by, in effect, extending the expansion up to the ϵ^2 term. This is what we mean when saying that we have used a more accurate approximation.

2. *Bhabha formulation*

For the Bhabha cross section, we can write the exact correction in Eq. (7) as a finite power series in the fractional energy loss ϵ (cf. Ref. 12)

$$c_B(\epsilon)=\sum_{i=-1}^{2}a_n\epsilon^n\ , \tag{33}$$

where the coefficients a_n are

$$\begin{aligned}a_{-1}&=\frac{\gamma^2-1}{\gamma^2}[(\gamma+1)^{-2}-2]\ ,\\ a_0&=\left[\frac{\gamma-1}{\gamma}\right]^2[(\gamma+1)^{-2}+3]\ ,\\ a_1&=\frac{-2(\gamma-1)^3}{\gamma(\gamma+1)^2}\ ,\end{aligned} \tag{34}$$

and

$$a_2=\frac{(\gamma-1)^4}{\gamma^2(\gamma+1)^2}\ .$$

If we insert this series into the Bhabha correction factor I_C^B defined by Eq. (24) then, using the table of integrals from the Appendix, it is straightfoward (but tedious) to derive

$$I_C^B=\frac{1}{\zeta}\left[b_{-1}\ln\frac{u}{\zeta}+\sum_{n=0}^{3}b_n\left[\frac{\zeta}{u}\right]^n\right]\ , \tag{35}$$

where, as before, $u=\zeta p$ and the b_n are defined in terms of the a_n of Eq. (34) by

$$\begin{aligned}b_{-1}&=\zeta a_{-1}\ ,\\ b_0&=\zeta(a_{-1}\Gamma+a_0+\tfrac{1}{2}a_1+\tfrac{1}{3}a_2)\ ,\\ b_1&=-\zeta a_0\ ,\\ b_2&=-\zeta a_1\ ,\end{aligned} \tag{36}$$

and

$$b_3 = -2\zeta a_2 \ .$$

Note that Eq. (35), the correction term for the Bhabha cross section, has been cast *in exactly the same form* as the Møller correction of Eq. (31), with only the substitution of the coefficients b_n for m_n. The results for the Møller cross section are obtained by using the same techniques as described below for the Bhabha case with merely a replacement of coefficients.

Inserting I_C^B from Eq. (35) into Eq. (25) leads to the following result:

$$\Phi(\lambda,\zeta)=\frac{1}{2\pi i}\int_{\sigma-i\infty}^{\sigma+\infty}\exp\left[\lambda u+u\ln u-b_{-1}\ln\frac{u}{\zeta}-\sum_{n=0}^{3}b_n\left[\frac{\zeta}{u}\right]^n\right]du \ . \tag{37}$$

To evaluate this integral we follow closely the analysis for the Rutherford cross section carried out by Börsch-Supan.[11] First make the trivial substitution $u=\sigma+iy$. Then we choose the saddle point for the Rutherford case $\sigma=e^{-(\lambda+1)}$. Finally (here we deviate from Ref. 11) we make another change of variable $y=-\ln q$. As it must, the imaginary part of the integral vanishes. After much algebra we find

$$\Phi(\lambda,\zeta)=\frac{1}{\pi}e^{-(\sigma+b_0)}\zeta^{b_{-1}}\int_0^1 J_q^{(1)}dq \ , \tag{38}$$

where

$$J_q^{(1)}=q^{-(T_S+1)}\frac{S_Q^{\sigma/2}}{S_L^{b_{-1}/2}}\exp\left[-\frac{\zeta}{S_L}\left[b_1\sigma+b_2\zeta\frac{S_F}{S_L}+b_3\sigma\zeta^2\frac{S_T}{S_L^2}\right]\right]$$

$$\times\cos\left\{L_Q\left[\frac{1}{2}\ln S_Q-1+\frac{\zeta}{S_L}\left[b_1+2b_2\zeta\frac{\sigma}{S_L}+b_3\zeta^2\frac{Q_T}{S_L^2}\right]\right]+T_S(\sigma-b_{-1})\right\} \ , \tag{39}$$

and the symbols in Eq. (39) have the following meanings:

$$\begin{aligned}
&L_Q=\ln q \ ,\\
&L_S=\frac{L_Q}{\sigma} \ ,\\
&S_L=\sigma^2+L_Q^2 \ ,\\
&S_Q=1+L_S^2=\frac{S_L}{\sigma^2} \ ,
\end{aligned} \tag{40}$$

$$\begin{aligned}
&T_S=\tan^{-1}L_S \ ,\\
&S_F=\sigma^2-L_Q^2 \ ,\\
&S_T=\sigma^2-3L_Q^2 \ ,
\end{aligned}$$

and

$$Q_T=3\sigma^2-L_Q^2 \ .$$

Unfortunately, our work is not yet complete. Consider the simple case where all $b_n=0$, i.e., the Rutherford case. Figure 2 shows the integrand $J_q^{(1)}$ plotted for two values of λ. Evidently $J_q^{(1)}$ is well behaved for small λ but wildly oscillatory for large values. Thus we limit the application of Eq. (38) to the range $\lambda<\lambda_c$, where λ_c is some critical value to be determined.

For large λ, it is convenient to avoid the branch cut in the integrand of Eq. (37) by choosing as a path the infinite semicircle in the negative real plane, as in Ref. 11. After a change of variables we find

$$\Phi(\lambda,\zeta)=-\frac{1}{\pi}e^{-b_0}\zeta^{b_{-1}}\int_0^1 J_q^{(2)}dq \ , \tag{41}$$

where

$$J_q^{(2)}=q^{(\lambda-1+\ln L_Q)}(-L_Q)^{-b_{-1}}e^{-Z_Q(b_1+b_2Z_Q+b_3Z_Q^2)}\sin[\pi(L_Q-b_{-1})] \ , \tag{42}$$

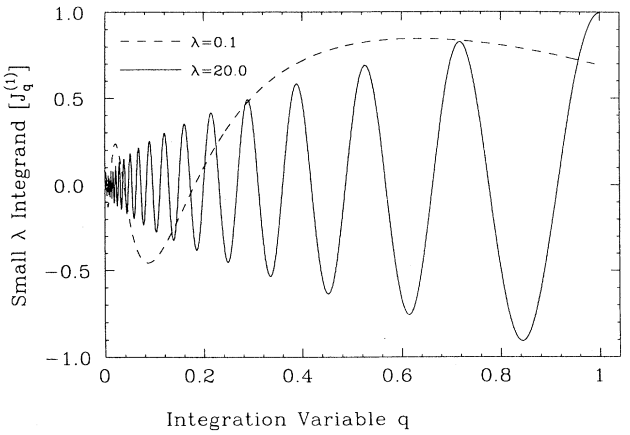

FIG. 2. Integrand $J_q^{(1)}$ from Eq. (39) plotted for $\lambda=0.1$ and 20. The oscillatory behavior for large λ necessitates a different numerical method for that region.

and

$$Z_Q=\frac{\zeta}{L_Q} . \tag{43}$$

The symbol L_Q has the same meaning as defined in Eq. (40).

The integrand $J_q^{(2)}$ is well behaved for large λ (see Fig. 3). From experimentation, a good value for the critical λ delimiting the two regions was found to be $\lambda_c \approx 0.2$. The small and large λ formulations gave identical results in the neighborhood of λ_c. Again, we emphasize that the analysis for the Bhabha cross section, culminating in the integrals of Eqs. (38) and (41), is equally applicable for Møller scattering if all b_n are replaced by the m_n of Eq. (32).

III. RESULTS

The numerical calculations were performed using the computer code LASPE,[13] which uses a binary tree driven Gaussian quadrature integration routine. In this section we describe some of the results we obtained. Many of the results reported here are for the case of a 450-MeV beam incident on a 0.1-gm/cm^2 thick target of ^{208}Pb, which corresponds to $\zeta=1.35\times10^{-5}$. This value is typical of modern experiments.

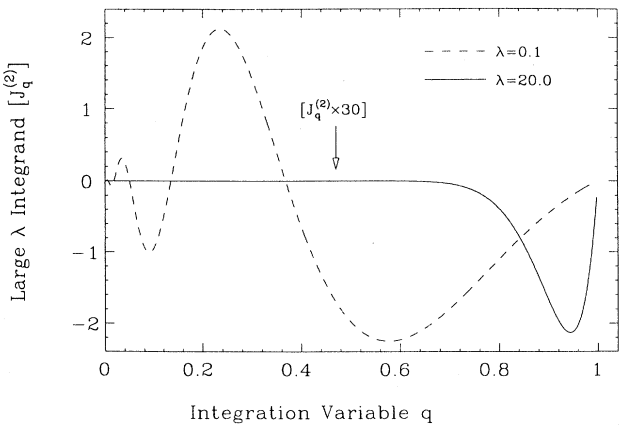

FIG. 3. Integrand $J_q^{(2)}$ from Eq. (42) plotted for $\lambda=0.1$ and 20. This integrand is well behaved for large λ.

A. Δ_{MP}, the most-probable energy loss, and W, the width of the straggling distribution

As mentioned previously, it is of interest to see how the approximations for the most-probable energy-loss Δ_{MP} and the distribution W differ from the Rutherford results of Eqs. (22) and (23). Also, we would like to compare our results with those of Rohrlich and Carlson[7] who investigated the problem using approximations for the Møller and Bhabha cross sections.

To compare with Rohrlich and Carlson, we assume forms similar to those found in their paper

$$\Delta_{MP}^{\pm}\approx\zeta\left[\ln\frac{\zeta}{\epsilon'}+0.198-a^{\pm}\nu\right] \tag{44}$$

and

$$W^{\pm}\approx\zeta(4.02-\alpha^{\pm}\mu) , \tag{45}$$

where

$$\alpha^{+}=\zeta\beta^2[2-(\gamma-1)^{-2}]$$

and

$$\alpha^{-}=\zeta\frac{2\gamma-1}{\gamma^2} . \tag{46}$$

The values of ν and μ, assumed by Rohrlich and Carlson to be constants, are to be determined from the calculated straggling distributions. The only difference from the Rohrlich and Carlson forms is that they use the incorrect constant in the expression for Δ_{MP} taken from the original Landau paper.

Figures 4 and 5 summarize the results of a series of calculations of electron and positron distributions for ener-

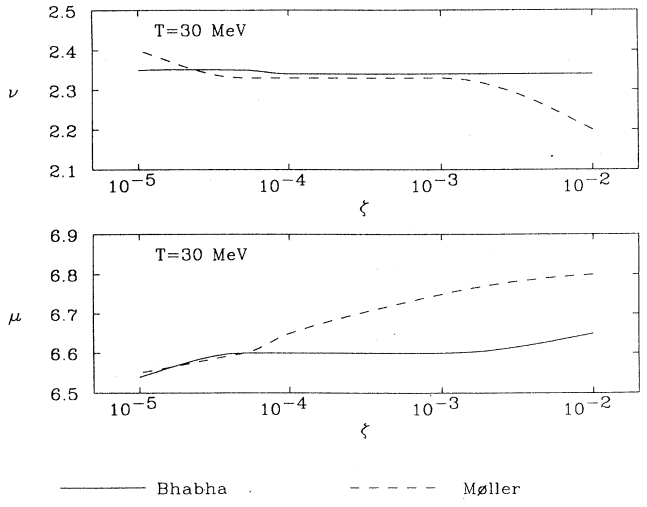

FIG. 4. Variation of ν and μ with respect to ζ for a constant energy $T=30$ MeV.

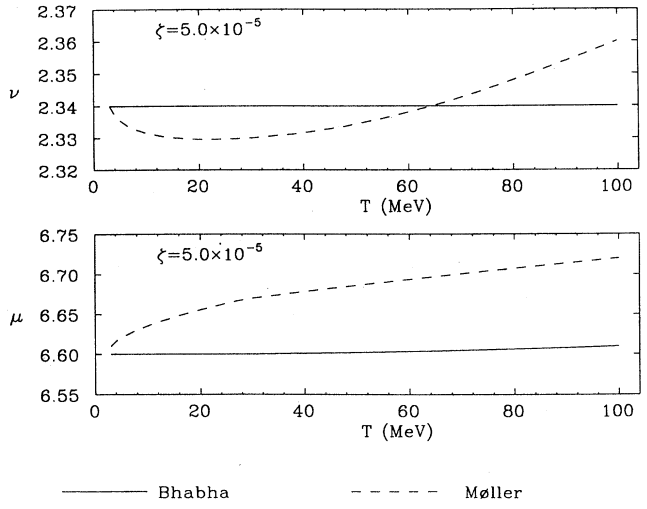

FIG. 5. Variation of ν and μ with respect to energy for a constant $\zeta=5.0\times10^{-5}$.

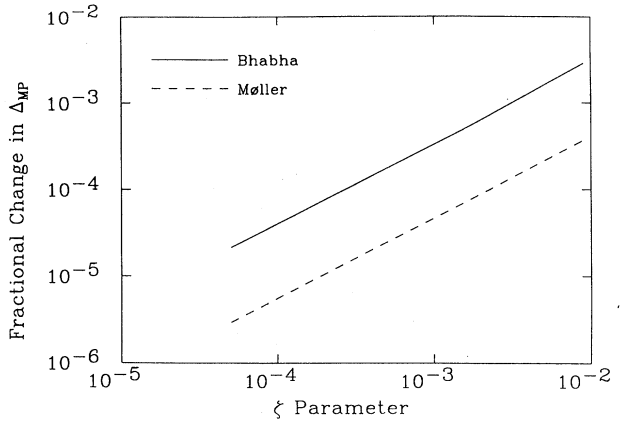

FIG. 7. The fractional change (from the Rutherford values) of the most-probable energy loss. Note that for the same value of ζ, the fractional change in Δ_{MP} is about ten times smaller than the change in the width.

gies ranging from 3 to 450 MeV and varying the target thickness such that ζ ranges from 10^{-5} to 10^{-2}. As can be seen from the figures, ν and μ are approximately constant over a broad range of parameter values of interest for typical electron scattering experiments. We were able to determine best-fit values of

$$\nu=2.34\pm0.08\ ,$$
$$\mu=6.62\pm0.09\ . \tag{47}$$

These results should be sufficient for any forseeable application. The result for μ is in agreement with Rohrlich and Carlson.[7] Comparing values of ν however, is problematic due to their use of an incorrect constant in the expression for Δ_{MP}.

The fractional change in the FWHM, W of the straggling distribution from the Rutherford value is shown in Fig. 6. Note that as ζ increases T decreases (for fixed x). Modern-day experiments tend to fall on the left half of the abscissa. A similar plot of the fractional change in the most-probable energy loss, Δ_{MP} is shown in Fig. 7. Note that for a given value of ζ, the fractional change in Δ_{MP} is about an order-of-magnitude smaller than the change in the width.

Figures 6 and 7 provide the first indication that for small values of ζ the results for the straggling distribution calculated using the Møller cross section are indistinguishable from those calculated by Landau using the Rutherford cross section. This result can be understood by examining the relativistic limit of the cross sections. In the remainder of this work, we will place greater emphasis on Rutherford-Bhabha differences.

B. Straggling distribution differences

A plot of the difference in the straggling distributions for the Rutherford and Bhabha cross sections for $\zeta=1.35\times10^{-5}$ is shown in Fig. 8. To appreciate the magnitude of this curve, the ordinate scale should be compared with that in Fig. 1. Not marked on the plot is

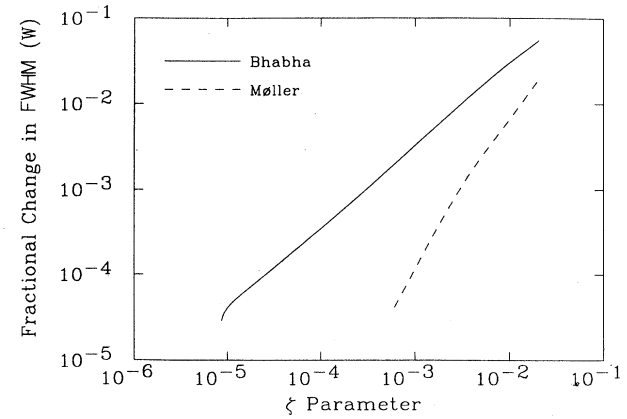

FIG. 6. The fractional change (from the Rutherford values) of the distribution width. Note that for small ζ the Møller results become indistinguishable from the Rutherford case.

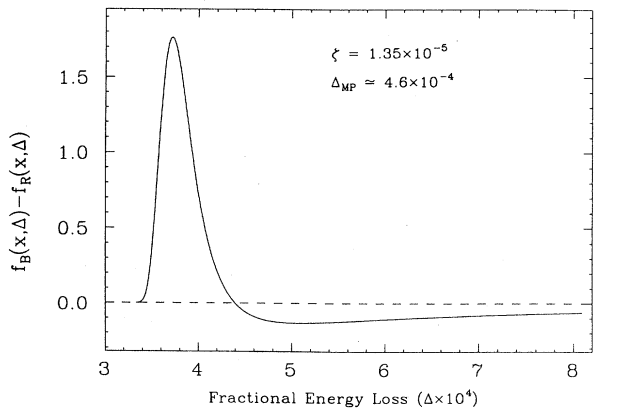

FIG. 8. Differences in the straggling distributions between 450-MeV electrons and positrons incident on ^{208}Pb ($x=0.1$ gm/cm^2).

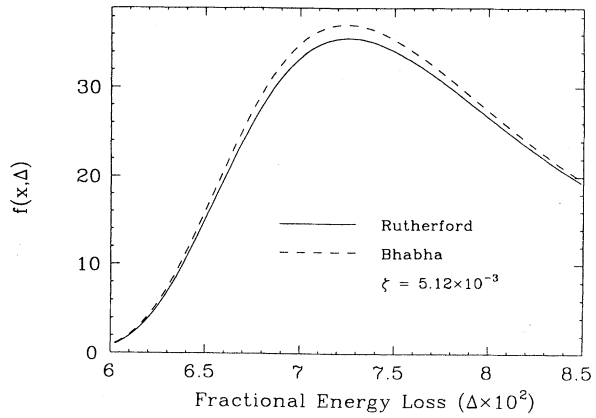

FIG. 9. A particular example of the comparison between the Rutherford and Bhabha distribution near the peak. The value of $\zeta=5.12\times10^{-3}$ corresponds (in this case) to a 3-MeV beam incident on ^{208}Pb with $x=0.25$ gm/cm^2.

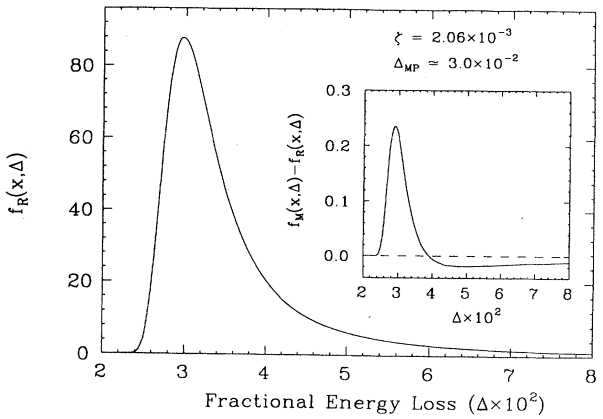

FIG. 11. Differences in the Rutherford and Møller straggling distributions for a 3-MeV electron incident on ^{208}Pb ($x=0.1$ gm/cm^2).

$\Delta_{MP}\approx4.6\times10^{-4}$, which falls very near to the energy loss at which the difference curve changes sign. Note that the curve in Fig. 8 must integrate to zero if both straggling distributions are correctly normalized.

In Fig. 9, we plot the distributions near the vicinity of the peak (for a thicker target and a much lower beam energy corresponding to $\zeta=5.12\times10^{-3}$). Note that the peak for the Bhabha distribution is enhanced relative to the Rutherford result; this effect is also evident (on a much smaller scale) for the case of $\zeta=1.35\times10^{-5}$ shown in Fig. 8. Also note that in examining Fig. 9 it is not apparent that the width for the Bhabha distribution is smaller, as given by Eq. (45), since it is not easy to compare the widths visually when the two curves have different maxima. In Fig. 10, we show the tail region of these same distributions; the increase in height of the Bhabha distribution near the peak is compensated by a decrease in this region, as must be the case if the distributions are correctly normalized.

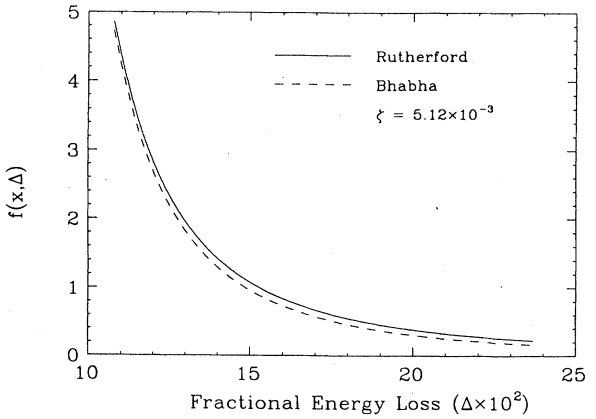

FIG. 10. A particular example of the comparison between the Rutherford and Bhabha distribution in the tail region. The value of $\zeta=5.12\times10^{-3}$ corresponds (in this case) to a 3-MeV beam incident on ^{208}Pb with $x=0.25$ gm/cm^2.

The results shown in Figs. 8–10 are general in the sense that for any choice of beam-target parameters for which this analysis is valid, the qualitative nature of the curves will not change. The Bhabha distribution will always have a smaller width, be enhanced in the vicinity of the peak, and be quenched in the tail region. Finally, we point out that differences between the Rutherford and Møller distributions are too small to be perceivable in Fig. 8.

To see the effect of the difference between the Møller and Rutherford cross sections, we must go to much larger values of ζ, corresponding to much lower beam energies. In Fig. 11 we show the Rutherford-Møller differences for the case of a 3-MeV incident beam.

C. Rutherford-Bhabha $\Psi(\lambda)$ differences

Data analysis programs that use the radiative correction technique to determine the total cross section require tables of values for the function $\Psi(\lambda)$ defined by

$$\Psi(\lambda)=\int_{\lambda}^{\infty}\Phi(\lambda,\zeta)d\lambda\ , \tag{48}$$

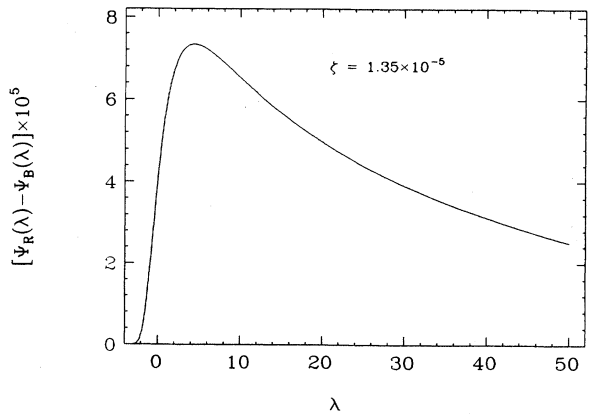

FIG. 12. Example of the change in the function $\Psi(\lambda)$, which is often used in data analysis programs.

where we have omitted reference to the explicit weak ζ dependence in Ψ. This function represents the total fraction of particles which have lost due to straggling a fractional energy greater than the Δ corresponding to λ [Δ and λ are related by Eq. (20)].

In Fig. 12, we plot a curve of the difference between Rutherford and Bhabha values of $\Psi(\lambda)$ for $\zeta=1.35\times10^{-5}$. Note that the effect on $\Psi(\lambda)$ of using the Bhabha rather than the Rutherford cross section is quite small. The peak of Fig. 12 occurs at $\lambda\approx4.5$. By consulting a table of $\Psi(\lambda)$ values we known that $\Psi(4.5)\approx0.2473$. Thus, for the case shown in Fig. 12, the fractional difference $(\Psi_R-\Psi_R)/\Psi_R$ near the peak is only about 0.03%.

IV. CONCLUSIONS

We have found approximations for the most-probable energy loss and the straggling distribution width summarized by Eqs. (44)–(47), which are applicable over a broad dynamical range of interest. For most applications of electron scattering, especially in the medium to high energy regimes, differences between the straggling distributions derived from the Rutherford and Møller cross sections are negligible. Data analysts can continue to use the Rutherford based Landau distributions without concern. For positron beams at intermediate energies, the deviation of the Bhabha based straggling distribution from Landau distribution, while still small, is more significant than in the Møller case. It may be necessary to take into account such differences, especially in experiments designed to measure small effects such as the dispersion correction differences between electron and positron scattering.

ACKNOWLEDGMENTS

It is a pleasure to acknowledge the helpful comments and suggestions of Professor Larry Cardman. This work was supported by the National Science Foundation under Grant No. NSF PHY86-10493.

APPENDIX: TABLE OF INTEGRALS

The following integral results are easy to derive. In keeping with the spirit of Landau's analysis, we have neglected terms $\mathcal{O}(\epsilon_1 p)$ and the exponential $e^{-p\epsilon_{\max}}$.

$$\int_{\epsilon_1}^{\epsilon_{\max}}\frac{1}{\epsilon}(1-e^{-p\epsilon})d\epsilon\approx\ln p\epsilon_{\max}+\Gamma\ ,$$

$$\int_{\epsilon_1}^{\epsilon_{\max}}(1-e^{-p\epsilon})d\epsilon\approx\frac{1}{p}(p\epsilon_{\max}-1)\ ,$$

$$\int_{\epsilon_1}^{\epsilon_{\max}}\epsilon(1-e^{-p\epsilon})d\epsilon\approx\frac{1}{p^2}[\tfrac{1}{2}(p\epsilon_{\max})^2-1]\ ,$$

$$\int_{\epsilon_1}^{\epsilon_{\max}}\epsilon^2(1-e^{-p\epsilon})d\epsilon\approx\frac{1}{p^3}[\tfrac{1}{3}(p\epsilon_{\max})^3-2]\ .$$

*Current address: Department of Physics and Computer Science, Newport News, VA 23606.

[1]L. Landau, J. Phys. (Moscow) **8**, 201 (1944).
[2]H. Bichsel, Rev. Mod. Phys. **60**, 663 (1988).
[3]G. H. Rawitscher, Phys. Rev. **151**, 846 (1966).
[4]G. H. Rawitscher, Massachusetts Institute of Technology Report No. MIT-2098-470, 1967 (unpublished).
[5]D. G. Ravenhall and R. L. Mercer, private communication.
[6]Saclay experiment proposal 161; L. S. Cardman, private communication.
[7]F. Rohrlich and B. C. Carlson, Phys. Rev. **93**, 38 (1954).
[8]R. M. Sternheimer, in *Methods of Experimental Physics,* edited by L. C. L. Yuan and C. S. Wu (Academic, New York, 1961), Vol. 5, Pt. A, pp. 13 and 14.
[9]H. A. Bethe, *Handbuch für Physik* (Springer, Berlin, 1933), p. 273.
[10]H. D. Maccabee and D. G. Papworth, Phys. Lett. **30A**, 241 (1969).
[11]W. Börsch-Supan, J. Res. Nat. Bur. Stand. **65B**, 245 (1961).
[12]J. M. Jauch and F. Rohrlich, *The Theory of Photons and Electrons,* 2nd ed. (Springer-Verlag, New York, 1976).
[13]D. P. Heddle (unpublished).